Title

Conserved Cysteine Residues Provide a Protein-Protein Interaction Surface in Dual Oxidase (DUOX) Proteins*

Journal

Journal of Biological Chemistry, 288(10)

ISSN

0021-9258

Authors

Meitzler, Jennifer L
Hinde, Sara
Bánfi, Botond
et al.

Publication Date

2013-03-01

DOI

10.1074/jbc.m112.414797

Peer reviewed

THE JOURNAL OF BIOLOGICAL CHEMISTRY VOL. 288, NO. 10, pp. 7147–7157, March 8, 2013
Published in the U.S.A.

Conserved Cysteine Residues Provide a Protein-Protein Interaction Surface in Dual Oxidase (DUOX) Proteins*

Received for publication, August 29, 2012, and in revised form, January 26, 2013 Published, JBC Papers in Press, January 29, 2013, DOI 10.1074/jbc.M112.414797

Jennifer L. Meitzler[‡], Sara Hinde[§], Botond Bánfi[§¶], William M. Nauseef[§], and Paul R. Ortiz de Montellano[‖1]

From the [‡]Laboratory of Molecular Pharmacology of the Center for Cancer Research, NCI, National Institutes of Health, Bethesda, Maryland 20892, the [§]Inflammation Program, Department of Medicine, and [¶]Department of Anatomy and Cell Biology, Roy J. and Lucille A. Carver College of Medicine, University of Iowa, and Veterans Administration Medical Center, Iowa City, Iowa 52240, and the [‖]Department of Pharmaceutical Chemistry, University of California, San Francisco, California 94158

Background: Dual oxidases (DUOXs) are membrane-bound ROS-generating enzymes.
Results: Conserved DUOX cysteines localized in an N-terminal domain contribute to enzymatic maturation, independent of structural stabilization.
Conclusion: Intermolecular disulfides support the interaction between DUOX enzymes and their maturation factors.
Significance: This study reflects a complex profile of protein interactions required for activity and localization of the DUOX enzymes.

Intramolecular disulfide bond formation is promoted in oxidizing extracellular and endoplasmic reticulum compartments and often contributes to protein stability and function. DUOX1 and DUOX2 are distinguished from other members of the NOX protein family by the presence of a unique extracellular N-terminal region. These peroxidase-like domains lack the conserved cysteines that confer structural stability to mammalian peroxidases. Sequence-based structure predictions suggest that the thiol groups present are solvent-exposed on a single protein surface and are too distant to support intramolecular disulfide bond formation. To investigate the role of these thiol residues, we introduced four individual cysteine to glycine mutations in the peroxidase-like domains of both human DUOXs and purified the recombinant proteins. The mutations caused little change in the stabilities of the monomeric proteins, supporting the hypothesis that the thiol residues are solvent-exposed and not involved in disulfide bonds that are critical for structural integrity. However, the ability of the isolated hDUOX1 peroxidase-like domain to dimerize was altered, suggesting a role for these cysteines in protein-protein interactions that could facilitate homodimerization of the peroxidase-like domain or, in the full-length protein, heterodimeric interactions with a maturation protein. When full-length hDUOX1 was expressed in HEK293 cells, the mutations resulted in decreased H_2O_2 production that correlated with a decreased amount of the enzyme localized to the membrane surface rather than with a loss of activity or with a failure to synthesize the mutant proteins. These results support a role for the cysteine residues in intermolecular disulfide bond formation with the DUOX maturation factor DUOXA1.

Cysteine residues often play essential roles in protein structure and function by conferring stability through disulfide bond formation, maintaining proper maturation and localization through protein-protein intermolecular interactions, or providing a thiol group for reactions with molecular substrates (1). Intramolecular disulfide bond formation, favored in oxidizing extracellular and endoplasmic reticulum (ER)[2] compartments, provides structural support for native function and localization; disulfide loss can cause mistargeting or malfunction of receptors and transporters (2, 3). The mammalian peroxidases are a protein family whose rigid structure is defined by a conserved set of disulfide bonds (*e.g.* six in myeloperoxidase (MPO), seven in lactoperoxidase (LPO)) (4–6). These heme-containing enzymes, which catalyze the H_2O_2-dependent oxidation of halide and pseudohalide ions to form antimicrobial agents in phagocytes, are a critical element of the human innate immune system (7). MPO is the only member of the known mammalian peroxidases that is functional as a native homodimer linked through a disulfide bond (4, 8). This MPO oligomerization gives rise to an unusually high stability (T_m >80 °C) that is important for its physiological role. More recently, a distinct family of proteins has been identified with members that are related to the mammalian peroxidases by sequence comparisons. The NADPH oxidase (NOX)/dual oxidase (DUOX) membrane proteins are expressed in various epithelial cells and produce reactive oxygen species (ROS). In humans, two members of the NOX family of proteins, hDUOX1 and hDUOX2, contain a domain that is related by sequence to the mammalian peroxidases.

The function of the peroxidase-like domain of the two DUOX isoforms remains unclear. Although sequence identities establish a similarity to the mammalian peroxidases, the DUOX proteins lack some of the residues that in the peroxidases are known to be required for heme binding and catalytic function.

* This work was supported by National Institutes of Health Grants DK 30297 (to P. R. O. M.), HL 090830 (to B. B.), and AI 70958 and AI 044642 (to W. M. N.). This work was also supported by the resources and use of facilities at the Iowa City Department of Veterans Affairs Medical Center, Iowa City, IA (to W. M. N.).

[1] To whom correspondence should be addressed: University of California, Genentech Hall GH-N572D, 600 16th St., San Francisco, CA 94158-2517. Tel.: 415-476-2903; Fax: 415-502-4728; E-mail: ortiz@cgl.ucsf.edu.

[2] The abbreviations used are: ER, endoplasmic reticulum; ABTS, 2,2′-azino-bis(3-ethylbenzothiazoleline-6-sulfonic acid; βME, β-mercaptoethanol; DUOX, dual oxidase; LPO, lactoperoxidase; MPO, myeloperoxidase; NOX, NADPH oxidase; ROS, superoxide + H_2O_2.

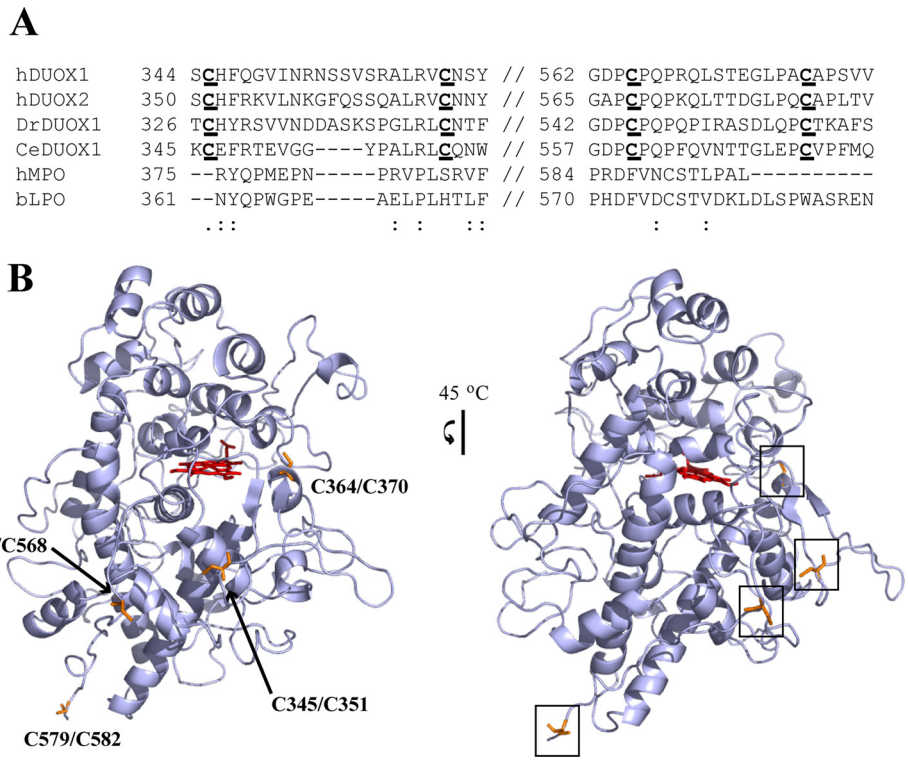

FIGURE 1. **Comparison of sequence and structural localization of critical cysteine residues in hDUOX isoforms.** *A*, sequence alignment of classic peroxidase domains with the hDUOX proteins. The *highlighted* segments shown focus on the regions encompassing the cysteine residues under study: Cys^{345}/Cys^{351}, Cys^{364}/Cys^{370}, Cys^{565}/Cys^{568}, Cys^{579}/Cys^{582} (hDUOX1/hDUOX2). *B*, structural model of $hDUOX2_{1-599}$ produced by the SWISS-MODEL program server and PyMOL. *Left*, view of model structure highlighting residues investigated by point mutation in *orange*. *Right*, 45-degree *y* axis rotation of the model structure, illustrating residue solvent exposure and localization along one plane of the DUOX protein structure.

Because the peroxidase-like domain is the salient difference between the DUOX enzymes and other members of the NOX family, it may be responsible for the fact that the DUOX enzymes produce H_2O_2, whereas the majority of the NOX family enzymes produce superoxide. Recent structural investigation of H_2O_2 producer NOX4 has revealed a unique large extracellular E-loop that may trap superoxide to allow conversion to H_2O_2, akin to the potential role of the DUOX N-terminal domain (9). Close analysis of the DUOX peroxidase-like region reveals the absence of the conserved cysteines known to confer structural stability to the mammalian peroxidases. Of the cysteine residues present in this region (seven for $hDUOX1_{1-593}$, six for $hDUOX2_{1-599}$), none corresponds by sequence alignment to a conserved disulfide pair in the mammalian peroxidases (Fig. 1*A*). The role of the cysteine residues that are present in the DUOX peroxidase-like region has recently been examined. Individual missense mutations of four of the cysteines in hDUOX2 (Cys^{351}, Cys^{370}, Cys^{568}, Cys^{582}) result in retention of the protein in the ER compartment, as observed by carbohydrate remodeling, indicating that these residues are critical to proper maturation (1, 10). It was speculated that the cysteines maintain a stable, N-terminal domain structure which, upon mutation, may cause misfolding and aggregation in the ER compartment. Further study demonstrated that the immature hDUOX2 is still capable of oxidant production (9). As this implies the cysteines may promote a critical protein-protein interaction rather than serving a structural function, we have modeled the N-terminal region of hDUOX2 to determine the approximate location of each of the cysteines (Fig. 1*B*). Modeling of the structure indicated that the thiol groups are solvent-exposed and unlikely to form intramolecular disulfide bonds due to the predicted distances between the cysteine residues.

To obtain greater insight into the role of these cysteines in DUOX structure and function, we mutated each of four cysteine residues in both the hDUOX1 and hDUOX2 isolated peroxidase-like domains. Our experiments with these purified mutant constructs established that the mutations cause little change in the stability of the monomeric unit, in agreement with the hypothesis that these cysteine residues are solvent-exposed and do not form intramolecular disulfide bonds. However, the ability of the isolated hDUOX1 peroxidase-like domain to dimerize was affected, and the mutated full-length holoproteins did not support normal oxidant production when expressed as stable transfectants. Taken together, these findings suggest a role for these cysteines, and perhaps the surface of the domain in which they are located, in contributing to protein-protein interactions.

EXPERIMENTAL PROCEDURES

Materials, Facilities, and General Instrumentation—Sf9 cells (Invitrogen) were grown in ExCell 420™ medium (SAFC Biosciences) supplemented with glutamine (2.7 g/liter). High Five™ cells were grown in Express Five™ medium (Invitrogen) supplemented with glutamine (2.7 g/liter) and 10% fetal bovine serum (FBS). Both cell lines were kept in suspension at 27 °C (100 rpm) and maintained at densities between 0.5×10^6 and 2×10^6 cells/ml. Human embryonic kidney 293 (HEK) cells (ATCC CRK01573) were purchased from the American Type

TABLE 1
Primers for mutations of hDUOX1$_{1-593}$ and hDUOX2$_{1-599}$

Mutation	Primer	Mutation	Primer
DX1_C345G_F	5′-catgagaaatgccagcGgccacttcc-3′	DX2_C351G_F	5′-gagaaatgccagcGgtcatttccggaaggtcc-3′
DX1_C345G_R	5′-ggaagtggcCgctggcatttctcatg-3′	DX2_C351G_R	5′-ggaccttccggaaatgacCgctggcatttctc-3′
DX1_C364G_F	5′-gctctccgggtcGgcaacagctactgg-3′	DX2_C370G_F	5′-cccaagctctcagggtcGgcaacaactactgg-3′
DX1_C364G_R	5′-ccagtagctgttgcCgacccggagagc-3′	DX2_C370G_R	5′-ccagtagttgttgcCgaccctgagagcttggg-3′
DX1_C565G_F	5′-ggcataaaggagaccccGgtccgcagccgag-3′	DX2_C568G_F	5′-ggtgcacccGgccctcaacctaagcagc-3′
DX1_C565G_R	5′-ctcggctgcggacCggggtctcctttatgcc-3′	DX2_C568G_R	5′-gctgcttaggttgagggcCgggtgcacc-3′
DX1_C579G_F	5′-gaaggcctgccagcgGgtgctccctctg-3′	DX2_C579G_F	5′-cggcctgccccagGgtgcacccctgac-3′
DX1_C579G_R	5′-cagagggagcacCcgctggcaggccttc-3′	DX2_C579G_R	5′-gtcaggggtgcacCctggggcaggccg-3′

Culture Collection (Manassas, VA) and maintained in Dulbecco's modified Eagle's medium/Ham's nutrient mixture F-12 medium that was supplemented with 10% FBS, 100 μg/ml streptomycin, 10 mM HEPES, and 2 mM L-glutamine. Diamide, H_2O_2 (30% w/w), and ABTS were purchased from Sigma-Aldrich. T4 DNA ligase and restriction endonucleases were obtained from New England Biolabs. DNA sequencing was performed by Elim Biopharmaceuticals and the DNA Sequencing Facility at the University of Iowa. The entire gene insert was completely sequenced for each plasmid construct. For protein identification, mass spectra from trypsin digestion were obtained on a QSTAR-XL hybrid QqTOF mass spectrometer (Applied Biosystems). Spectrophotometric measurements were performed on a Cary 50 Bio UV-visible spectrophotometer (Varian). For experiments utilizing H_2O_2, concentrations were determined spectrophotometrically at 240 nm by using the molar extinction coefficient $\epsilon = 43.6\ M^{-1}\ cm^{-1}$ (11). All experiments were performed at room temperature unless otherwise stated.

Structure Prediction—The hDUOX2 protein was truncated using the TMHMM transmembrane helix algorithm to identify the primary sequence that composes the N-terminal peroxidase-like domain (12). A structural model of hDUOX2$_{1-599}$ was built by sequence submission to the SWISS-MODEL program server for automatic modeling; the model with bovine LPO (Protein Data Bank ID code 3BXI) as the template was visualized with the software PyMOL (13). Heme co-factor placement in the model structure was achieved by overlay of the known bovine LPO structure and the hDUOX2$_{1-599}$ homology model.

Plasmid Constructs—The peroxidase-like domain constructs for hDUOX1 (residues 1–593) and hDUOX2 (residues 1–599) were described previously (14, 15). Briefly, the original source of the *Homo sapiens duox1$_{1-593}$* gene was Quick-clone cDNA from human lung (Clontech). The gene encoding the peroxidase-like domain of hDUOX1 (residues 1–593) was PCR-amplified and inserted by ligation into pAcGP67-b (pJLM08). *hduox2$_{1-599}$* was synthesized by GeneArt Inc. and was subcloned from the GeneArt vector into pAcGP67-b baculovirus expression vector (named pJLM025). Both plasmid constructs for hDUOX peroxidase-like domain expression encode a C-terminal His$_6$ tag to aid protein purification.

Mutations in *hduox1$_{1-593}$* were introduced into pJLM05 (14) by QuikChange site-directed mutagenesis (Clontech), according to the manufacturer's instructions. Primer sequences are listed in Table 1. The entire open reading frame was resequenced for each new plasmid. Each plasmid construct was subsequently digested with BamHI and EcoRI, and the gene(s) were inserted by ligation into pAcGP67-b (WT, pJLM08; C345G, pJLM072; C364G, pJLM073; C565G; pJLM074; and C579G, pJLM075). Mutations in *hduox2$_{1-599}$* were introduced utilizing the same approach as *hduox1$_{1-593}$*; primer sequences are also listed in Table 1 (WT, pJLM025; C351G, pJLM084; C370G, pJLM085; C568G, pJLM086; and C582G, pJLM087).

The hDUOX1 and hDUOXA1 HEK293 expression constructs were generated as follows. Total RNA was extracted from well differentiated primary cultures of human airway epithelial cells and reverse transcribed using Thermoscript. The coding regions of human DUOX1 and DUOXA1 transcripts were amplified by PCR using HiFi DNA polymerase (Invitrogen) and the primers listed in Table 2. Amplification of hDUOX1 also depended on the presence of Q-solution (Qiagen; 0.5× final concentration) in the PCR buffer. The PCR products were cloned into the TOPO-TA vector (Invitrogen), sequenced, and then subcloned between the NotI and BamHI sites of the pcDNA3.1 mammalian expression vector (Invitrogen).

Generation of Recombinant Baculoviruses—Plasmids (pJLM08, pJLM025, pJLM072–75, and pJLM084–87) were co-transfected with viral baculogold DNA into Sf9 insect cells, according to the manufacturer's instructions (BD Biosciences). The resulting viruses were plaque-assayed to generate high titer recombinant baculovirus stocks amplified (two rounds of amplification in Sf9 cells) from single viral populations.

Expression and Purification of hDUOX Proteins—All hDUOX1$_{1-593}$ and hDUOX2$_{1-599}$ constructs were expressed and purified according to the previously reported procedure (14). Briefly, 1 liter of High Five cells (2.0×10^6 cells/ml) supplemented with 250 μM 5-aminolevulinic acid (Fluka) was infected with the hDUOX1$_{1-593}$-His$_6$ viral stock at a multiplicity of infection of 5 for 3 days at 27 °C. After 72 h of infection, cell suspensions were concentrated and purified by nickel affinity chromatography (nickel-nitrilotriacetic acid-agarose at 4 °C, in phosphate buffer (20 mM phosphate, 400 mM NaCl, pH 8.0)). The purified proteins were stored at −20 °C, and all stock concentrations were determined in triplicate by Bradford assay (16).

Tryptophan Fluorescence Spectroscopy—The fluorescence emission spectra of DUOX1$_{1-593}$ Cys mutants were collected at 20 °C using a Fluorolog 3 Spectrofluorometer (Horiba Jobin Yvon), with excitation at 292 nm. Emission was monitored between 315 and 450 nm using an excitation band width of 8 nm, with slit widths set at 2.5 nm for pH 4.0 and pH 7.0 spectra. Wavelength maxima achieved for the hDUOX1$_{1-593}$ constructs were 341 nm (pH 4.0) and 348 nm (pH 7.0), consistent with previously published data for wild-type hDUOX1$_{1-593}$ (15).

TABLE 2
Primers for isolation of hDUOX1 and hDUOXA1 for HEK293 expression constructs

Construct	Primer
hDUOX1 Forward	5′-gcggccgccaccatgggcttctgcctggctcta-3′
hDUOX1 Reverse	5′-ggatcctctgctcaactggacagtgg-3′
hDUOXA1 Forward	5′-gcggccgccaccatggctactttgggacacacattc-3′
hDUOXA1 Reverse	5′-ggatccgcctccacggggaggaatgtta-3′

Evaluation of hDUOX Secondary Structure—Far-UV circular dichroism (CD) spectra were collected on a JASCO J-815 spectropolarimeter using a cuvette path length of 1.0 mm and spectral collection in the range of 195–260 nm. All 20 °C CD experiments were conducted in 10 mM phosphate buffer, at pH 7.0 at a protein concentration of 4 μM. Temperature gradient spectra were collected at a concentration of 3 μM in 10 mM phosphate buffer, pH 7.0, over a temperature range of 20–60 °C; increasing at 2 °C/min, CD data were collected every 5 ° after 30 s of temperature stability. Raw ellipticity data were converted to mean residue ellipticity before plotting.

Creation of Stable HEK Transfectants—Mutated regions of the peroxidase-like domain of hDUOX1 were digested with restriction enzymes and inserted into the full-length hDUOX1 in pcDNA3.1(+) Zeo (from Invitrogen). Stable HEK cell lines were created as done previously (17, 18); HEK cells already stably transfected with hDUOXA1 were transfected with mutant plasmids using the Qiagen PolyFect Transfection Reagent according to the manufacturer's procedure. Stable transfectants were selected with stepwise concentrations of zeomycin (100–250 μg/ml) and cloned.

Gel Filtration Analysis of hDUOX1 and hDUOX2 Proteins—Proteins were subjected to gel filtration on a Superdex 200 10/300 column (Amersham Biosciences) equilibrated with 20 mM phosphate, 400 mM NaCl buffer, pH 8.0. Fifty microliters of each protein (40 μM) was separated at 0.5 ml/min at 4 °C and compared with gel filtration standards (Bio-Rad 151-1901) injected after reconstitution according to the manufacturer's instructions. Protein elution was monitored by the absorbance at 280 nm.

Reduction and Oxidation of $hDUOX1_{1-593}$—The hDUOX1 peroxidase-like domain (5 μM) was incubated with 200 mM β-mercaptoethanol (βME) in 20 mM phosphate buffer, 400 mM NaCl, pH 8.0 (4 °C) for reduction. Partial reduced protein was retained for gel analysis; reducing agent was removed from the remaining protein by sequential dilution and concentration (3×, 1:40 sample:buffer). The resulting protein was incubated at room temperature for 30 min, treated with diamide (100 μM), or untreated. All samples were loaded on SDS-PAGE for analysis.

Hydrogen Peroxidase Production by HEK Transfectants—For measurement of oxidant production, 5×10^4 wild-type or hDUOX1/hDUOXA1 cells were cultured overnight in 96-well microtiter plates. Before the assay, medium was gently removed and replaced with phosphate buffer saline (pH 7.4) containing 10 mM glucose. H_2O_2 production by wild-type HEK cells or hDUOX1 transfectants was measured as horseradish peroxidase-dependent (1 unit/ml) peroxidation of Amplex Red (50 μM) at 37 °C. Amplex Red peroxidation was monitored continuously at 550 nm and the amount of H_2O_2 produced calculated from a standard curve (0–5 nmol). The concentration of the stock H_2O_2 used to generate the standard curve was determined spectrophotometrically, using an extinction coefficient 43.6 M^{-1} cm^{-1} at 240 nm. In all cases, measurements of Amplex Red peroxidation were performed in triplicate.

Biosynthesis of DUOX1—Stable HEK transfectants expressing wild-type or mutant hDUOX1 with hDUOXA1 were grown in T-75 flasks and suspended in methionine-free RPMI 1640 medium with 10% dialyzed FBS and antibiotics for 1 h before biosynthetic radiolabeling, as done previously (17, 18). 25 μCi of [^{35}S]methionine (EasyTagEXPRESS protein labeling mix, >37 TBq/mmol; Perkin-Elmer) was added, and cells were biosynthetically radiolabeled for 2 h. Cells were harvested or subjected to a chase with unlabeled methionine (100 mM) for 18 h. Cells were harvested by centrifugation and solubilized as described previously. Human DUOX1 was immunoprecipitated using a rabbit polyclonal antibody (ab106544; Abcam), and samples were separated by SDS-PAGE followed by autoradiography. Amounts of radioisotopically labeled hDUOX1 were quantitated using a PhosphorImager (Typhoon 9410; Amersham Biosciences).

RESULTS

Sequence Comparison of Peroxidase Domains Reveals That DUOX Cysteine Residues Contribute Little to Structural Stability—Cysteine residues, which are the most reactive natural amino acids due to their oxidatively susceptible thiol group, play important roles in modifying the structure and function of many proteins. Cysteine oxidation to disulfide bonds provides structural stability to many enzymes, including the mammalian peroxidases MPO and LPO, which utilize a conserved disulfide network to maintain an α-helix-rich motif. Due to the sequence and structural similarities of the DUOX peroxidase-like domain with the mammalian peroxidases, we reasoned that a comparison of the conserved structural features between these proteins might uncover important differences essential to functionality. Recently, the abundance of cysteines within the DUOX2 N-terminal region was the focus of mutagenesis experiments that suggested a role for these residues in the maturation of the DUOX proteins (1, 10, 19). To clarify the role of the cysteines, a sequence alignment analysis was performed that focused on the four cysteine residues that resulted in stalled maturation (Fig. 1*A*). These cysteine residues are conserved across the DUOX proteins of both lower and higher organisms, emphasizing their importance to the DUOX system. This alignment also illustrates the lack of conservation of cysteine residues between the DUOX proteins and the mammalian peroxidases, suggesting that, in contrast to MPO or LPO, these residues may not constitute a disulfide network that maintains structural integrity.

Each cysteine residue was mapped onto a structural model of the DUOX2 N-terminal region ($DUOX2_{1-599}$; Fig. 1*B*). Our previous analysis of the DUOX peroxidase-like domains ($hDUOX1_{1-593}$ and $hDUOX2_{1-599}$) showed the greatest amino acid variation to occur at the exposed extracellular face (15), a feature that may promote recognition of different interacting proteins. Each cysteine residue was found to exist as a solvent-exposed residue, situated on one face of the protein surface.

```
SolhDUOXA2   -EWFVGTVNTNTSYKAFSAARVTARVGLLVGLEGINITLTGTPVHQLNETIDYNEQFTWR 133
SolmDUOXA2   AEWFVGTVNTNTSYKAFSAARVTARVRLLVGLEGINITLTGTPVHQLNETIDYNEQFTWR 133
SolhDUOXA1   -EWSVGQVSTNTSYKAFSSEWISADIGLQVGLGGVNITLTGTPVQQLNETINYNEEFTWR 133
SolmDUOXA1   -EWSVGHVNANTTYKAFSPKWVSVDVGLQIGLGGVNITFTGTPVQQLNETINYNEAFAWR 133
              ** ** *.:**:*****.  ::. : * :** *:***:*****:******:*** *:**

SolhDUOXA2   LKENYAAEYANALEKGLPDPVLYLAEKFTPSSPCGLYHQYHL-------- 175
SolmDUOXA2   LKENYAAEYANALEKGLPDPVLYLAEKFTPSSPCGLYHQYHL-------- 175
SolhDUOXA1   LGENYAEEYAKALEKGLPDPVLYLAEKFTPRSPCGLYRQYRLAGHYTSAM 183
SolmDUOXA1   LGRSYAEEYAKALEKGLPDPVLYLAEKFTPRSPCGLYNQYRLAGHYAS-- 181
             * ..** ***:****************** ******.**:*
```

FIGURE 2. **Partial alignment of the DUOX maturation factors.** The sequence alignment shown, generated by the ClustalW program, encompasses the soluble domain of DUOX maturation factors from both human (*h*) and mouse (*m*). Soluble domains were determined by the TMHMM 2.0 Server; SolhDUOXA1: 75–183 AA, SolhDUOXA2: 75–175, SolmDUOXA1: 75–181, SolmDUOXA2: 74–175. The conserved cysteine residues (Cys^{167}) found in both DUOXA1 and DUOXA2 are *highlighted* in *red*.

The closest distance between cysteines in hDUOX2 is predicted to be 14 angstroms, between Cys^{351} (hDUOX1 Cys^{345}) and Cys^{568} (hDUOX1 Cys^{565}), suggesting that none of these residues is involved in disulfide bonds for structural stabilization. Due to their solvent exposure and unlikely involvement in internal disulfide bonds, we postulated that these cysteine residues may enable protein-protein interactions that are required for maturation. Two DUOX maturation factor isoforms (DUOXA1 and DUOXA2) interact specifically with their corresponding DUOX isoform (21, 22). The interaction of these two protein pairs could occur through intermolecular disulfide bonds that bridge the DUOX peroxidase-like domain and a small extracellular DUOXA domain. Interestingly, a conserved cysteine, DUOXA1/A2 Cys^{167}, is found in both maturation factor domains (Fig. 2) (23). To explore the role(s) of the DUOX cysteine residues, they were individually mutated to glycines in both the truncated peroxidase-like domains and in the full-length DUOX proteins.

Mutations of the DUOX Peroxidase-like Domain(s) Causes Significant Changes in the SDS Mobility and Oligomerization State of the Isolated Region While Structural Integrity Is Maintained—To test the role of cysteine residues in the peroxidase domain, Cys^{345}/Cys^{351}, Cys^{364}/Cys^{370}, Cys^{565}/Cys^{568}, and Cys^{579}/Cys^{582} (hDUOX1/hDUOX2) were mutated to a glycine residue to mimic previous studies focused on hDUOX2, which suggested that membrane trafficking dysfunction was linked to these specific thiols as a result of protein misfolding (1). Each mutated DUOX protein was stably overexpressed in baculovirus and purified by nickel-nitrilotriacetic acid-agarose affinity chromatography, as reported previously for the wild-type protein (Fig. 3) (14). LC-tandem MS of the trypsin-digested hDUOX1 protein verified the presence of each mutated glycine residue. All of the purified proteins were obtained in amounts comparable with those of the wild-type domain, providing initial evidence that the cysteine residues are not essential for structural stability of the N-terminal domain. Further evidence that the mutant proteins retained overall structural integrity was provided by the absence of a notable shift in the Trp fluorescence maxima at either pH 4.0 or pH 7.0 (Fig. 3*A*). CD spectroscopy was performed to ascertain the relative stability of mutants *versus* wild-type protein under conditions of varied temperature (Fig. 3, *B* and *C*). At 20 °C, the CD profile of each mutant protein demonstrated a nearly identical CD profile to its wild-type peroxidase domain isoform. Perturbation by temperature gradient was performed for the mutation(s) that completely abolished maturation ($hDUOX1_{1-593}$ C579G and $hDUOX2_{1-599}$ C582G) and demonstrated similar profiles of unfolding and stability at the more physiologically relevant temperature of 35 °C (Fig. 3*C*). Heme titration of mutant constructs demonstrated no shift in the absorbance wavelength previously observed for the wild-type peroxidase-like domain, consistent with retention of a weak heme binding affinity (15).

Initial SDS-PAGE analysis of hDUOX1 protein constructs demonstrated a single band for each mutant under reducing conditions with 1.25% βME as the reductant (Fig. 3*D*, *top*, potential minor band from protein splicing observed for C364G only). Under nonreducing conditions, electrophoretic separation resulted in characteristic double band patterns composed of a high molecular mass (~60 kDa, completely reduced protein) and low molecular mass (~55 kDa, completely oxidized protein) band for each cysteine mutant. This effect has previously been observed in studies of human glucokinase and was linked to shifts in intramolecular disulfide bridges as a result of multiple cysteine interactions resulting in a more or less compact protein structure within the gel environment (24, 25). In our hands, each specific point mutation demonstrated a unique double band profile, perhaps due to differential disulfide bridging, though unlikely due to residue position.

Interestingly, a distinct protein at ~120 kDa was observed under nonreducing conditions for both the wild-type and mutant hDUOX1 constructs, with the Cys^{364} point mutation demonstrating the least amount (Fig. 3*D*, *top right panel*, *asterisk*). The presumed molecular mass of this species suggests that a portion of the hDUOX1 peroxidase domain is in a homodimeric state that is susceptible to change upon reduction, implying that the state is achieved through an intermolecular disulfide interaction. The same set of conserved cysteines was mutated in the peroxidase domain of hDUOX2 to establish whether any significant differences are observed and to further clarify the recently elucidated differing nature of the two DUOX isoforms (Fig. 3*D*, *bottom*) (15). Once again, each hDUOX2 protein demonstrates a monomeric band; however, differences were noted under nonreducing conditions. No band for dimeric association was noted for WT $hDUOX2_{1-599}$ whereas the C351G mutation demonstrates a band suggesting dimerization and/or oligomerization (Fig. 3*D*, *bottom right gel*).

Size Exclusion Chromatography Supports Dimerization, Specific to the hDUOX1 Peroxidase Domain—To support the SDS-PAGE analysis of each DUOX peroxidase domain with a solution-based experimental approach, wild-type $hDUOX1_{1-593}$

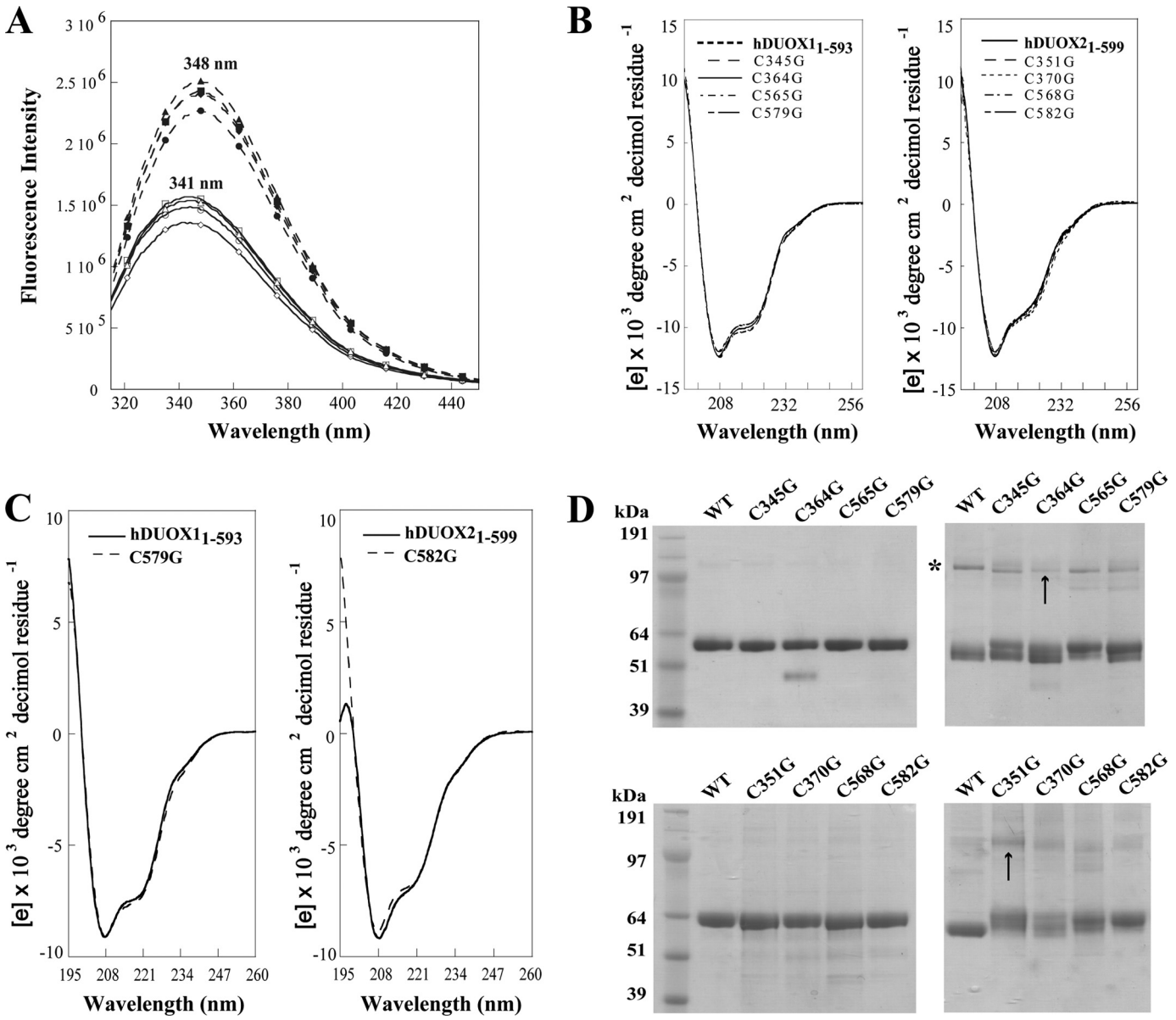

FIGURE 3. **Structural characterization of DUOX mutants.** *A*, tryptophan fluorescence emission spectra of DUOX1$_{1-593}$ cysteine mutants (C345G, *diamond*; C364G, *circle*; C565G, *square*; C579G, *triangle*), collected at 341 nm (pH 4.0, *solid line*) and 348 nm (pH 7.0, *dashed line*). *B*, CD spectra of hDUOX1$_{1-593}$ and hDUOX2$_{1-599}$ at 20 °C with their respective cysteine mutants compared at pH 7.0, with the spectra overlaid for comparison. *C*, CD spectral comparison of hDUOX1$_{1-593}$ *versus* C579G (*left*) and hDUOX2$_{1-599}$ *versus* C582G (*right*) at 35 °C, collected during temperature gradient studies. All CD experiments were conducted in 10 mM phosphate buffer. *D*, *top*, hDUOX1$_{1-593}$ cysteine mutants under reducing (*left*) and nonreducing (*right*) conditions. An *asterisk* highlights the upper proposed dimer band, seen to vary in intensity, most notably for C364G (*arrow*). *D*, *bottom*, hDUOX2$_{1-599}$ cysteine mutant set studied under reduced (*left*) and nonreduced (*right*) conditions. Obvious dimerization appears absent from wild-type and mutant proteins except for C351G (*arrow*).

was subjected to gel filtration analysis. Late eluting features, causing slight positive and negative deflections from 16 to 18 ml, were seen due to varying amount of glycerol in each sample relative to the elution buffer (26). With this technique two protein peaks were observed, suggesting multiple oligomeric states (Fig. 4). The apparent molecular masses of the peaks were determined to be 60.9 kDa for the second symmetrical peak (13.6 ml) and 133.3 kDa for the first peak at 11.9 ml. The mass of the second, evidently monomeric peak is consistent with the calculated molecular mass for hDUOX1$_{1-593}$ of 67.8 kDa. The first peak is close to the projected molecular mass for a dimeric hDUOX1 peroxidase domain of 135.6 kDa. The relative abundance of the dimeric species appears greater under solution phase conditions than observed via SDS-PAGE analysis, likely due to the absence of the SDS denaturant in the gel filtration study. Consistent with the polyacrylamide gel bands, the C345G, C565G, and C579G mutant proteins display slightly less dimeric protein than WT (data not shown), with C364G showing the least amount of dimeric species at a level approaching that of the fully reduced protein (Fig. 4*A*). hDUOX2$_{1-599}$ was also studied by size exclusion, to verify the unique absence of dimeric association observed with the hDUOX1 peroxidase domain. Injection of WT hDUOX2$_{1-599}$ (68.3 kDa) resulted in a monomeric peak eluting at the same volume as WT hDUOX1$_{1-593}$, consistent with their similarity in mass (Fig. 4, *A* and *B*). Low lying peaks were observed from a

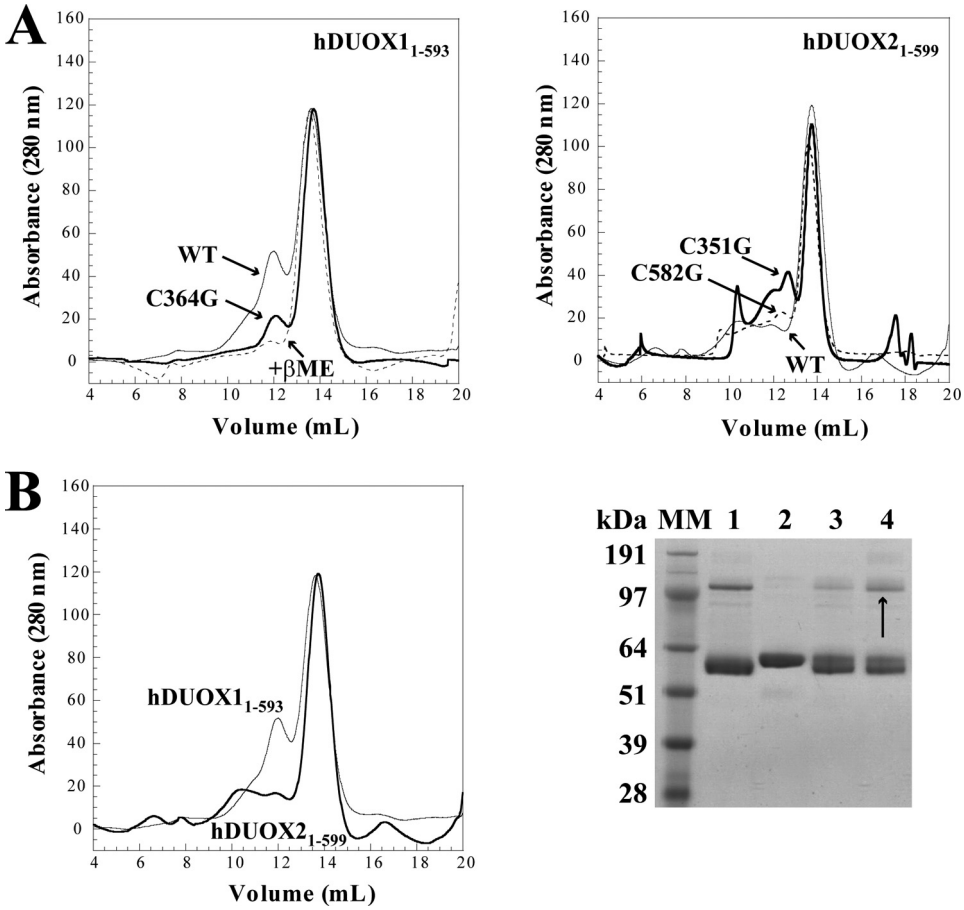

FIGURE 4. **Gel filtration analysis of DUOX truncated proteins.** *A*, comparison of hDUOX1$_{1-593}$ wild-type (*WT*), reduced (+*βME*), and C364G proteins (*left*) and hDUOX2$_{1-599}$ WT, C351G, and C582G (*right*). *Arrows* highlight the varying amounts of the dimeric species. *B*, direct comparison of hDUOX1$_{1-593}$ and hDUOX2$_{1-599}$ by size exclusion (*left*) and SDS-PAGE analysis (*right*) of hDUOX1$_{1-593}$ unreduced WT (*lane 1*) and reduced WT protein with *β*ME (*lane 2*). After reductant removal, incubation at room temperature without (*lane 3*) or with diamide addition (*lane 4*) demonstrated hDUOX1$_{1-593}$ dimer reformation.

retention volume of 9–12.5 ml, suggestive of some nonspecific oligomerization occurring, but a significant peak for dimeric protein was not observed. SDS-PAGE analysis had suggested the presence of dimeric species by a diffuse band observed with the mutant C351G; therefore, all hDUOX2$_{1-599}$ mutants were also analyzed by size exclusion. Of the mutant constructs, only C351G and C582G showed unresolved peaks at 12.5 ml (Fig. 4*A*), within a region of oligomerization, perhaps suggesting that mutation of these cysteine residues had produced a unique minor affinity between monomeric units; however, this does not appear to be significant or favor production of a specific new protein state. To further ascertain that the dimerization observed for the hDUOX1 peroxidase domain is in fact a native, stable complex and not a product of nonspecific association, the reversibility of dimerization after disruption by reduction was studied.

hDUOX1$_{1-593}$ Monomer/Dimer Conversion Investigated Utilizing Diamide Oxidation—Dimerization of the hDUOX1 peroxidase domain construct analyzed by both SDS-PAGE and gel filtration analysis together with the previously reported instability of the hDUOX1 construct compared with a more stable monomeric hDUOX2$_{1-599}$, argue for the *in vivo* relevance of this interaction (15). This evidence diminishes the likelihood of a nonspecific protein-protein interaction, and data collected for the C364G hDUOX1$_{1-593}$ mutated protein suggests dimerization occurs through a disulfide bond. To help support the specificity of this interaction and its direct association with thiol groups, a solution of purified hDUOX1$_{1-593}$ was fully reduced by exposure to *β*ME (Fig. 4*B*, *gel*). In this reduced state, as shown previously, no dimer was observed. The reduced protein was dialyzed extensively to remove the reducing agent and then incubated for 30 min at room temperature, with or without diamide to determine whether oxidation can return the protein to a dimeric state. Oxidation achieved by atmospheric exposure alone demonstrated a small amount of dimer, whereas dimerization was returned to levels observed prior to reduction with the thiol-specific oxidant diamide. This supports the hypothesis that disulfide bonds result in specific dimerization of hDUOX1$_{1-593}$ and demonstrates that protein reduction did not disrupt dimer formation through denaturation of the overall monomeric protein structure. Review of the structural models of each DUOX N-terminal region shows that Cys^{364} of hDUOX1 is solvent-exposed; however, the corresponding conserved cysteine of hDUOX2 (Cys^{370}) is partially buried and turned inward, suggesting that this cysteine may be unavailable for dimerization due to its position, in accord with our experimental results (Fig. 5).

Normal and Mutant DUOX1 Expression and Activity in Stable Transfectants—To determine how the mutation of specific extracellular cysteines influences the activity and cellular fate of

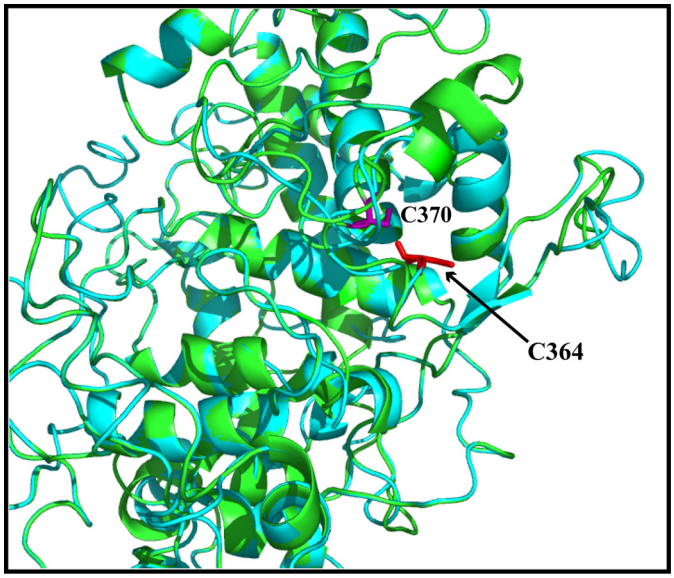

FIGURE 5. **Overlay of DUOX1 and DUOX2 peroxidase-like domain model structures.** The predicted structures of hDUOX1 (*cyan*) and hDUOX2 (*green*) N-terminal regions were overlaid to demonstrate the difference in the relative positions of the conserved cysteine residues Cys^{364} (*red*) of hDUOX1 and Cys^{370} (*purple*) of hDUOX2.

TABLE 3

Cysteine mutation effects on hDUOX1 system activity in stable transfectants

H_2O_2 production by wild-type and transfected cell lines stimulated with phorbol 12-myristate 13-acetate and ionomycin was quantitated spectrophotometrically as peroxidation of Amplex Red ($n = 8$). In parallel, the relative amounts of immunoreactive hDUOX1 protein in membrane-enriched fractions from HEK transfectants were assessed by immunoblotting; these data are expressed relative to levels in transfectants expressing normal hDUOX1.

Cell line	H_2O_2 production	Stable protein level
	nmol H_2O_2/5 × 10^4 cells in 2 h	*%*
Wild-type HEK cells	0.03 ± 0.01	
DUOX1/A1	2.12 ± 0.22	100
C345G/A1	0.16 ± 0.03	20.5
C364G/A1	0.64 ± 0.10	40.8
C565G/A1	0.15 ± 0.04	6.0
C579G/A1	0.04 ± 0.02	2.2

hDUOX1, we created stable HEK transfectants expressing wild-type and mutant hDUOX1 along with normal hDUOXA1. The agonist-dependent production of H_2O_2 was significantly depressed in lines expressing mutant hDUOX1 (Table 3), with the activity of C579G hDUOX1 essentially the same as that of nontransfected HEK cells.

Because reduced extracellular generation of H_2O_2 could reflect compromised production or subcellular targeting of mutant hDUOX1, as well as defective oxidase activity, we compared the biosynthesis of normal and mutant DUOX1 by pulse-chase radiolabeling (Fig. 6*A*). Immunoprecipitation of biosynthetically radiolabeled hDUOX1 demonstrated that all of the mutants were initially expressed at levels that exceeded ≥7-fold that of the wild-type protein (Fig. 6*B*). However, during the chase period, there was more rapid loss of mutant protein than of normal DUOX1, suggesting instability of the mutant proteins during processing and membrane targeting. Consistent with this interpretation, immunoblots of membrane-enriched fractions of wild-type and mutant hDUOX1/hDUOXA1 lines demonstrated reduced amounts of each of the mutants that paralleled the reduction in oxidase activity (Table 3). This observation implies that the protein fraction that reached the plasma surface was fully functional and that the effect of each mutation was to disrupt a protein association required for maturation, not to compromise structural stability or functionality of each enzyme.

DISCUSSION

The absence of critical cysteine residues in enzymatic systems due to mutation has been linked to protein trafficking disorders. Specifically, thyroid dysfunction resulting in goiters is associated with missense mutations of cysteines in the thyroglobulin gene that result in its retention in the ER (27, 28). Recently, cysteine mutations in the DUOX2 protein, a ROS-generating enzyme that is highly expressed in the thyroid, have also been reported to result in failed maturation from the ER (1, 10, 19). These studies have highlighted the importance of conserved thiol residues within the hDUOX2 N-terminal peroxidase-like domain for proper targeting to the plasma membrane.

The DUOX enzymes have structural and functional features that are atypical among members of the NOX protein family. Most notably, they possess a large, extracellular domain that has sequence similarity with mammalian peroxidases, and, akin to NOX4, their stimulation yields hydrogen peroxide as the detectable oxidant (29–32). Comprehensive characterization of the two membrane-bound isoforms has been hindered by the inability to purify the full-length enzyme, a limitation circumvented in part by structural and topology modeling of important features (14, 15, 33, 34). Here, we have utilized structure prediction to identify the location of four cysteine residues previously shown to be important for DUOX2 maturation, establishing both that they are likely to be solvent-exposed and that their spatial orientation places them beyond the limits of internal disulfide bond formation (Fig. 1*B*). We further characterized the role of these conserved residues, not only in hDUOX2 but also in hDUOX1, through point mutations. Replacement of these specific cysteine residues did not significantly affect the structural stability of the isolated domain, as assessed through protein production levels, tryptophan fluorescence, circular dichroism, and heme binding studies.

Replacement of Cys^{364} with a glycine disrupted the previously unrecognized self-association of the $hDUOX1_{1-593}$ N-terminal region. Gel analysis and size exclusion chromatography confirmed the homodimerization of the hDUOX1-truncated construct, a behavior not shared by the hDUOX2 peroxidase-like domain (Figs. 3 and 4). Dimerization is one means by which proteins confer stabilization; therefore the observed hDUOX1 complexation is consistent with our previous demonstration that the peroxidase-like hDUOX1 domain is less stable under neutral conditions than the N-terminal region of hDUOX2 (15). Perhaps hDUOX1 dimerization is required for stability to achieve the correct structure or interaction with its maturation factor, hDUOXA1. Further analysis of the hDUOX1 dimeric state through reductive disruption and oxidative recovery of the dimeric protein with a thiol-specific oxidant, diamide, supported the conclusion that this complexation

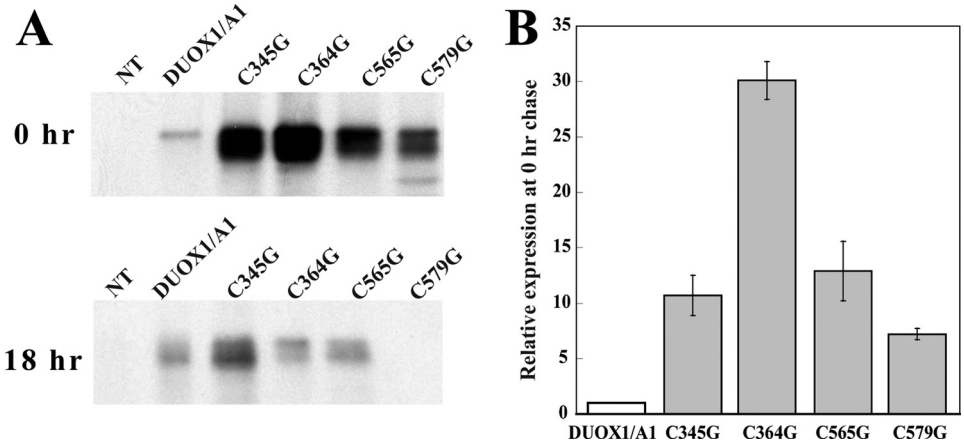

FIGURE 6. **Biosynthesis and activity of hDUOX1 mutants.** *A*, wild-type nontransfected HEK (*NT*) and transfected HEK cells expressing normal (hDUOX1/A1) or hDUOX1 mutants were pulse-labeled for 2 h, harvested (0 h chase), or chased (18 h) with cold methionine, and immunoprecipitated with anti-hDUOX1 antibody. Immunoprecipitates were separated by SDS-PAGE and subjected to autoradiography. DUOX1-related proteins were quantitated by a PhosphorImager. The gel is a representative of two independent experiments. *B*, amounts of radiolabeled mutant hDUOX1 were compared with the amount of normal hDUOX1 synthesized under the same conditions (0 h chase). Values are normalized to that for normal hDUOX1, and the data are the mean ± S.D. (*error bars*) for two independent pulse-chase experiments.

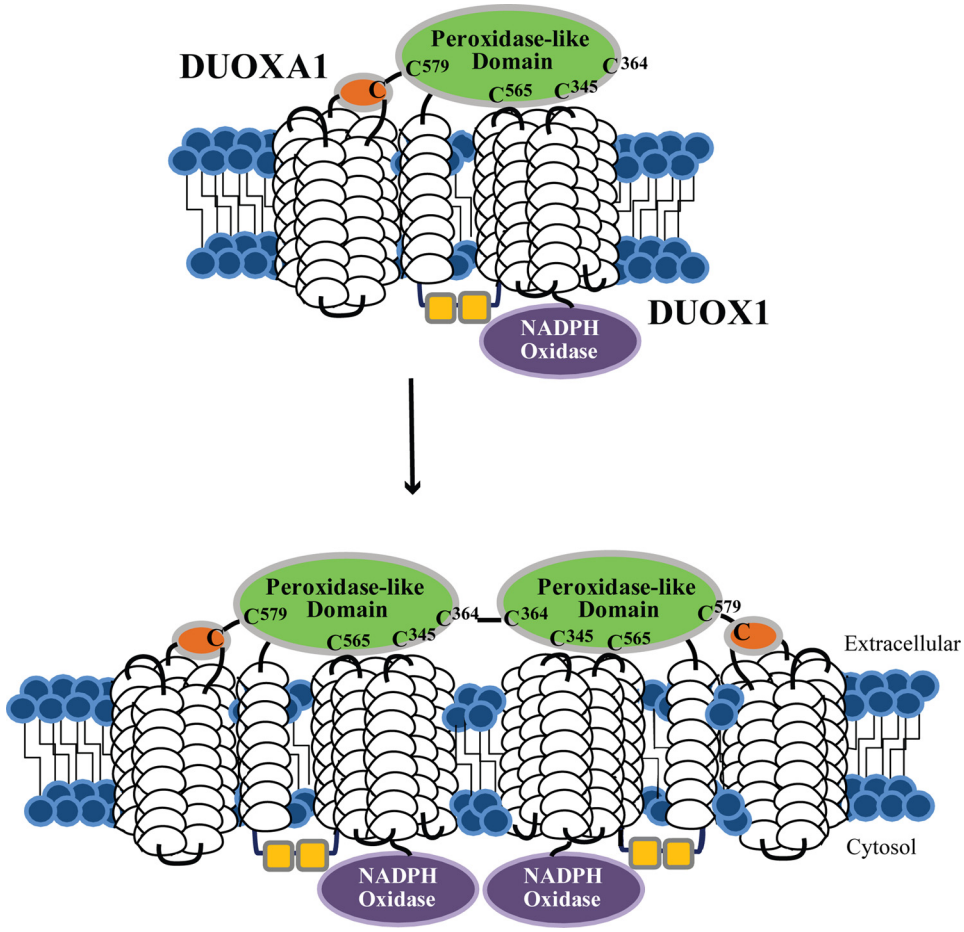

FIGURE 7. **Model of potential hDUOX1 protein and maturation factor association *in vivo*.** Interactions of the peroxidase-like domain of hDUOX1 (*green*) with both a soluble extracellular region of the hDUOXA1 maturation factor (*orange*) and itself are demonstrated. Cys^{345}, Cys^{364}, Cys^{565}, and Cys^{579} are *highlighted*, demonstrating their relative positions within the peroxidase-like domain of DUOX1. A potential disulfide bonding interaction may exist between a cysteine within the hDUOXA1 domain and a hDUOX1 cysteine (possibly Cys^{579}). The loss of *in vitro* dimerization upon mutation of Cys^{364} within the N-terminal region of hDUOX1 suggests that this residue was responsible for self-association of the hDUOX1 peroxidase-like domain through a disulfide interaction, illustrated here in the context of the full-length protein.

depends upon one or more disulfide bonds. Due to the sequence and structural similarities of the DUOX N-terminal region with those of the mammalian peroxidases, it is important to note that myeloperoxidase is capable of dimerizing through a disulfide bond to afford high structural stability (4, 8). Although it remains to be demonstrated in the context of the

full-length DUOX proteins, it is interesting to consider that dimerization may be one factor that differentiates the DUOX isoforms. Differences in dimerization could affect localization and functionality, as homodimerization is known to be required for function in certain enzymatic systems, including caspases, metalloproteins, and serine/threonine kinases (35–41). To test the possibility that dimerization may also play a role in the type of ROS detected, hDUOX1 HEK mutant transfectants, including C364G, were assayed for both hydrogen peroxide and superoxide production; however, no significant superoxide anion was detected (data not shown).

Investigation of the localization of HEK293 transfectants, both of full-length wild-type hDUOX1/A1 and full-length mutant hDUOX1 (C345G, C364G, C565G, and C579G)/A1 demonstrated defective membrane translocation, consistent with previous investigations in which conserved cysteines in hDUOX2 were mutated (1, 10). Our findings show that mutation of these cysteines did not disrupt the stability of the peroxidase-like region. Furthermore, analysis of the full-length system demonstrated that the level of hydrogen peroxide produced by mutant constructs correlated with the amount of stably expressed protein (Table 3), suggesting that these cysteine residues did not diminish activity, but only compromised maturation. These data support a model in which direct interaction of hDUOX1 and its hDUOXA1 maturation factor occurs through contact of cysteine residue(s) in their extracellular domains (Fig. 7). This protein-protein interaction surface is then perturbed by introduction of functionally inert glycine residues in positions previously occupied by cysteine thiols. The replacement of critical cysteine residues with glycine likely compromises proper folding of hDUOX1 as well, thus enlisting ER-associated degradation of misfolded precursors. Although the fate of mutant hDUOX1 that failed to associate with hDUOXA1 was not assessed in our studies, it is conceivable that without productive interactions with hDUOXA1 in the ER, some of the mutant hDUOX1 underwent degradation in the proteasome as part of the quality control system operative during protein synthesis. Such is the fate of Y173C, a specific missense mutation underlying one genotype of inherited MPO deficiency; pharmacologic inhibition of proteasome activity in cells expressing Y173C rescues the mutant protein from degradation, although it does not restore peroxidase activity in the cell (42).

We propose that the most important residue for interaction at the extracellular plane of hDUOX proteins is Cys^{579}/Cys^{582} (hDUOX1/hDUOX2), as it is the only residue whose mutation completely eliminates membrane trafficking. Other cysteines may form further contact points for stability within the full-length system, either with the maturation factor, or within the DUOX protein itself at the extracellular membrane spanning loops that lead to varied levels of disturbance to maturation. Previous studies have also demonstrated loss of DUOX-thyroid peroxidase association upon both introduction of the irreversible cysteine modification agent *N*-ethylmaleimide or single site mutations (10, 20). This suggests DUOX-thyroid peroxidase association is dependent upon cysteine interactions to stabilize the protein complex. Findings from this study also suggest the potential for homodimeric protein association for the hDUOX1 enzyme. Although confirmation is necessary in the context of the full-length system, it is possible that a disulfide-based interaction, either sustained or transient, is required to stabilize the hDUOX1 protein. This interaction may define yet another difference between the DUOX isoforms, as it was not observed for the more stable hDUOX2 protein.

Acknowledgments—We thank Karine Reiter and the Narum laboratory for the use of their JASCO J-815 spectropolarimeter. Mass spectrometric proteomic analyses were carried out by Bio-Organic Biomedical Mass Spectrometry Resource at the University of California (director, A. L. Burlingame) supported by National Center for Research Resources Grant P41RR001614.

REFERENCES

1. Morand, S., Agnandji, D., Noel-Hudson, M. S., Nicolas, V., Buisson, S., Macon-Lemaitre, L., Gnidehou, S., Kaniewski, J., Ohayon, R., Virion, A., and Dupuy, C. (2004) Targeting of the dual oxidase 2 N-terminal region to the plasma membrane. *J. Biol. Chem.* **279,** 30244–30251
2. Tarnow, P., Schoneberg, T., Krude, H., Gruters, A., and Biebermann, H. (2003) Mutationally induced disulfide bond formation within the third extracellular loop causes melanocortin 4 receptor inactivation in patients with obesity. *J. Biol. Chem.* **278,** 48666–48673
3. Hänggi, E., Grundschober, A. F., Leuthold, S., Meier, P. J., and St-Pierre, M. V. (2006) Functional analysis of the extracellular cysteine residues in the human organic anion transporting polypeptide, OATP2B1. *Mol. Pharmacol.* **70,** 806–817
4. Zeng, J., and Fenna, R. E. (1992) X-ray crystal structure of canine myeloperoxidase at 3 Å resolution. *J. Mol. Biol.* **226,** 185–207
5. Singh, A. K., Singh, N., Sharma, S., Singh, S. B., Kaur, P., Bhushan, A., Srinivasan, A., and Singh, T. P. (2008) Crystal structure of lactoperoxidase at 2.4 Å resolution. *J. Mol. Biol.* **376,** 1060–1075
6. Wolf, S. M., Ferrari, R. P., Traversa, S., and Biemann, K. (2000) Determination of the carbohydrate composition and the disulfide bond linkages of bovine lactoperoxidase by mass spectrometry. *J. Mass Spectrom.* **35,** 210–217
7. Klebanoff, S. J. (2005) Myeloperoxidase: friend and foe. *J. Leukoc. Biol.* **77,** 598–625
8. Banerjee, S., Stampler, J., Furtmüller, P. G., and Obinger, C. (2011) Conformational and thermal stability of mature dimeric human myeloperoxidase and a recombinant monomeric form from CHO cells. *Biochim. Biophys. Acta* **1814,** 375–387
9. Takac, I., Schröder, K., Zhang, L., Lardy, B., Anilkumar, N., Lambeth, J. D., Shah, A. M., Morel, F., and Brandes, R. P. (2011) The E-loop is involved in hydrogen peroxide formation by the NADPH oxidase Nox4. *J. Biol. Chem.* **286,** 13304–13313
10. Fortunato, R. S., Lima de Souza, E. C., Ameziane-el Hassani, R., Boufraqech, M., Weyemi, U., Talbot, M., Lagente-Chevallier, O., de Carvalho, D. P., Bidart, J. M., Schlumberger, M., and Dupuy, C. (2010) Functional consequences of dual oxidase-thyroperoxidase interaction at the plasma membrane. *J. Clin. Endocrinol. Metab.* **95,** 5403–5411
11. Hildebrandt, A. G., Roots, I., Tjoe, M., and Heinemeyer, G. (1978) Hydrogen peroxide in hepatic microsomes. *Methods Enzymol.* **52,** 342–350
12. Krogh, A., Larsson, B., von Heijne, G., and Sonnhammer, E. L. (2001) Predicting transmembrane protein topology with a hidden Markov model: application to complete genomes. *J. Mol. Biol.* **305,** 567–580
13. Arnold, K., Bordoli, L., Kopp, J., and Schwede, T. (2006) The SWISS-MODEL workspace: a web-based environment for protein structure homology modelling. *Bioinformatics* **22,** 195–201
14. Meitzler, J. L., and Ortiz de Montellano, P. R. (2009) *Caenorhabditis elegans* and human dual oxidase 1 (DUOX1) "peroxidase" domains: insights into heme binding and catalytic activity. *J. Biol. Chem.* **284,** 18634–18643
15. Meitzler, J. L., and Ortiz de Montellano, P. R. (2011) Structural stability and heme binding potential of the truncated human dual oxidase 2 (DUOX2) peroxidase domain. *Arch. Biochem. Biophys.* **512,** 197–203

16. Bradford, M. M. (1976) A rapid and sensitive method for the quantitation of microgram quantities of protein utilizing the principle of protein-dye binding. *Anal. Biochem.* **72,** 248–254
17. Goedken, M., McCormick, S., Leidal, K. G., Suzuki, K., Kameoka, Y., Astern, J. M., Huang, M., Cherkasov, A., and Nauseef, W. M. (2007) Impact of two novel mutations on the structure and function of human myeloperoxidase. *J. Biol. Chem.* **282,** 27994–28003
18. Loughran, N. B., Hinde, S., McCormick-Hill, S., Leidal, K. G., Bloomberg, S., Loughran, S. T., O'Connor, B., O'Fagáin, C., Nauseef, W. M., and O'Connell, M. J. (2012) Functional consequence of positive selection revealed through rational mutagenesis of human myeloperoxidase. *Mol. Biol. Evol.* **29,** 2039–2046
19. Ameziane-El-Hassani, R., Morand, S., Boucher, J. L., Frapart, Y. M., Apostolou, D., Agnandji, D., Gnidehou, S., Ohayon, R., Noël-Hudson, M. S., Francon, J., Lalaoui, K., Virion, A., and Dupuy, C. (2005) Dual oxidase-2 has an intrinsic Ca^{2+}-dependent H_2O_2-generating activity. *J. Biol. Chem.* **280,** 30046–30054
20. Song, Y., Ruf, J., Lothaire, P., Dequanter, D., Andry, G., Willemse, E., Dumont, J. E., Van Sande, J., and De Deken, X. (2010) Association of duoxes with thyroid peroxidase and its regulation in thyrocytes. *J. Clin. Endocrinol. Metab.* **95,** 375–382
21. Morand, S., Ueyama, T., Tsujibe, S., Saito, N., Korzeniowska, A., and Leto, T. L. (2009) DUOX maturation factors form cell surface complexes with DUOX affecting the specificity of reactive oxygen species generation. *FASEB J.* **23,** 1205–1218
22. Luxen, S., Noack, D., Frausto, M., Davanture, S., Torbett, B. E., and Knaus, U. G. (2009) Heterodimerization controls localization of DUOX-DUOXA NADPH oxidases in airway cells. *J. Cell Sci.* **122,** 1238–1247
23. Grasberger, H., and Refetoff, S. (2006) Identification of the maturation factor for dual oxidase: evolution of a eukaryotic operon equivalent. *J. Biol. Chem.* **281,** 18269–18272
24. Tiedge, M., Krug, U., and Lenzen, S. (1997) Modulation of human glucokinase intrinsic activity by SH reagents mirrors post-translational regulation of enzyme activity. *Biochim. Biophys. Acta* **1337,** 175–190
25. Tiedge, M., Richter, T., and Lenzen, S. (2000) Importance of cysteine residues for the stability and catalytic activity of human pancreatic beta cell glucokinase. *Arch. Biochem. Biophys.* **375,** 251–260
26. Kang, D. C., Venkataraman, P. A., Dumont, M. E., and Maloney, P. C. (2011) Oligomeric state of the oxalate transporter, OxlT. *Biochemistry* **50,** 8445–8453
27. Kim, P. S., Hossain, S. A., Park, Y. N., Lee, I., Yoo, S. E., and Arvan, P. (1998) A single amino acid change in the acetylcholinesterase-like domain of thyroglobulin causes congenital goiter with hypothyroidism in the cog/cog mouse: a model of human endoplasmic reticulum storage diseases. *Proc. Natl. Acad. Sci. U.S.A.* **95,** 9909–9913
28. Hishinuma, A., Takamatsu, J., Ohyama, Y., Yokozawa, T., Kanno, Y., Kuma, K., Yoshida, S., Matsuura, N., and Ieiri, T. (1999) Two novel cysteine substitutions (C1263R and C1995S) of thyroglobulin cause a defect in intracellular transport of thyroglobulin in patients with congenital goiter and the variant type of adenomatous goiter. *J. Clin. Endocrinol. Metab.* **84,** 1438–1444
29. De Deken, X., Wang, D., Many, M. C., Costagliola, S., Libert, F., Vassart, G., Dumont, J. E., and Miot, F. (2000) Cloning of two human thyroid cDNAs encoding new members of the NADPH oxidase family. *J. Biol. Chem.* **275,** 23227–23233
30. Martyn, K. D., Frederick, L. M., von Loehneysen, K., Dinauer, M. C., and Knaus, U. G. (2006) Functional analysis of Nox4 reveals unique characteristics compared to other NADPH oxidases. *Cell. Signal.* **18,** 69–82
31. Serrander, L., Cartier, L., Bedard, K., Banfi, B., Lardy, B., Plastre, O., Sienkiewicz, A., Fórró, L., Schlegel, W., and Krause, K. H. (2007) NOX4 activity is determined by mRNA levels and reveals a unique pattern of ROS generation. *Biochem. J.* **406,** 105–114
32. Geiszt, M., Witta, J., Baffi, J., Lekstrom, K., and Leto, T. L. (2003) Dual oxidases represent novel hydrogen peroxide sources supporting mucosal surface host defense. *FASEB J.* **17,** 1502–1504
33. Edens, W. A., Sharling, L., Cheng, G., Shapira, R., Kinkade, J. M., Lee, T., Edens, H. A., Tang, X., Sullards, C., Flaherty, D. B., Benian, G. M., and Lambeth, J. D. (2001) Tyrosine cross-linking of extracellular matrix is catalyzed by DUOX, a multidomain oxidase/peroxidase with homology to the phagocyte oxidase subunit $gp91^{phox}$. *J. Cell Biol.* **154,** 879–891
34. Leto, T. L., Morand, S., Hurt, D., and Ueyama, T. (2009) Targeting and regulation of reactive oxygen species generation by Nox family NADPH oxidases. *Antioxid. Redox Signal.* **11,** 2607–2619
35. Riedl, S. J., Fuentes-Prior, P., Renatus, M., Kairies, N., Krapp, S., Huber, R., Salvesen, G. S., and Bode, W. (2001) Structural basis for the activation of human procaspase-7. *Proc. Natl. Acad. Sci. U.S.A.* **98,** 14790–14795
36. Chen, M., Orozco, A., Spencer, D. M., and Wang, J. (2002) Activation of initiator caspases through a stable dimeric intermediate. *J. Biol. Chem.* **277,** 50761–50767
37. Renatus, M., Stennicke, H. R., Scott, F. L., Liddington, R. C., and Salvesen, G. S. (2001) Dimer formation drives the activation of the cell death protease caspase 9. *Proc. Natl. Acad. Sci. U.S.A.* **98,** 14250–14255
38. Koo, B. H., Kim, Y. H., Han, J. H., and Kim, D. S. (2012) Dimerization of matrix metalloproteinase-2 (MMP-2): Functional implication in MMP-2 activation. *J. Biol. Chem.* **287,** 22643–22653
39. Günther, V., Davis, A. M., Georgiev, O., and Schaffner, W. (2012) A conserved cysteine cluster, essential for transcriptional activity, mediates homodimerization of human metal-responsive transcription factor-1 (MTF-1). *Biochim. Biophys. Acta* **1823,** 476–483
40. Constantinescu Aruxandei, D., Makbul, C., Koturenkiene, A., Lüdemann, M. B., and Herrmann, C. (2011) Dimerization-induced folding of MST1 SARAH and the influence of the intrinsically unstructured inhibitory domain: low thermodynamic stability of monomer. *Biochemistry* **50,** 10990–11000
41. Singh, M., Kumar, P., and Karthikeyan, S. (2011) Structural basis for pH dependent monomer-dimer transition of 3,4-dihydroxy 2-butanone-4-phosphate synthase domain from *Mycobacterium tuberculosis*. *J. Struct. Biol.* **174,** 374–384
42. DeLeo, F. R., Goedken, M., McCormick, S. J., and Nauseef, W. M. (1998) A novel form of hereditary myeloperoxidase deficiency linked to endoplasmic reticulum/proteasome degradation. *J. Clin. Invest.* **101,** 2900–2909